

# The Role of Processing in the Fabrication and Optimization of Plastic Solar Cells

By Jeffrey Peet, Michelle L. Senatore, Alan J. Heeger,\* and Guillermo C. Bazan\*

The development of high-efficiency plastic solar cells is rapidly accelerating as the need for economically viable alternative energy sources becomes evident. Polymer-based bulk-heterojunction (BHJ) solar cells are attractive in that they can be coated from solution onto flexible substrates by a variety of techniques and thus inexpensive large-volume manufacturing should be possible. Further, the inherent flexibility of the polymeric materials combined with thin photovoltaic active layers results in devices that can be adapted to a variety of unique aesthetics and form factors. Recent advances in key relationships between thin-film casting methods, bulk-heterojunction morphology, and device performance have occurred in tandem with the synthesis of novel polymer semiconductors that possess increased optical-absorption breadth and optoelectronic performance. This Research News article highlights a few techniques developed to optimize the BHJ nanomorphology and performance of solar cells fabricated by various solution-processing methods.

the path forward will require simultaneous optimization of interrelated parameters to achieve the performance necessary to compete with existing technologies. Recent efforts to determine the maximum obtainable solar-power conversion efficiencies for solution-processed devices have estimated that solar-power conversion efficiencies (PCE) in excess of 10% for a single layer device and 15% for a tandem device are feasible.<sup>[3,4]</sup> These theoretical numbers are based on known loss factors and realistic device parameters for devices fabricated by solution-casting techniques, and thus represent levels of performance that could realistically be achieved with new materials and innovative processing techniques.

New materials will have to be combined with a more-fundamental understanding of the optimal device nanostructure and the

specific effects of various processing parameters on solar-cell performance to achieve significantly higher efficiencies. While the properties of conventional inorganic semiconductors can be predicted with some degree of precision, and device performance is closely related to the material purity and crystalline-domain size, the factors contributing to the performance of relatively disordered organic electronic devices are numerous and difficult to isolate. Even the effects of intermolecular structure and processing on the performance of one of the simplest and most-widely studied organic semiconductors, pentacene, have proven exceedingly complex.<sup>[5,6]</sup> The transition from a sublimed small-molecule film to a solution-cast polymer film adds significant complexity, due to the more electronically and conformationally complex polymer backbone, the pendant alkyl groups used to solubilize the polymer, and the less-controlled film-formation method. BHJ solar cells utilize an absorbing layer that consists of a solution-cast blend of a light-absorbing polymeric electron donor and a fullerene-based electron acceptor. The fundamental concept of the BHJ solar cell can be stated in a few words: nanoscale phase separation of the donor and acceptor components leads to charge-separating heterojunctions throughout the bulk of the thin-film composite material. Separated carriers then move toward the electrodes on bicontinuous interpenetrating networks. The morphology of the phase separation is therefore critical; it simultaneously enables both charge separation and collection. The blend phase diagram and the corresponding miscibility between the two components is

## 1. Introduction

Polymer BHJ solar cells have the potential to be highly efficient, economically competitive, and conceptually straightforward to integrate into our existing infrastructure.<sup>[1]</sup> While the solar-power conversion efficiencies and operational lifetimes are not yet competitive with inorganic solar cells, the potential for large-scale production of high-performance photovoltaics using continuous printing or coating techniques has created significant excitement among scientists and engineers in academic and commercial laboratories. Unlike most traditional solar-cell systems, BHJ solar cells can be fabricated from a wide range of materials with different aesthetic and optoelectronic properties by a diverse set of processes.<sup>[1,2]</sup> This results in a unique versatility in device form factor and functionality, which will enable performance optimization and consumer applications beyond simple rooftop and solar-farm installations; however, that same versatility means that

[\*] Prof. A. J. Heeger, Prof. G. C. Bazan, J. Peet, M. L. Senatore  
Center for Polymers and Organic Solids  
University of California at Santa Barbara  
Santa Barbara, California, 93106 (USA)  
E-mail: ajhe@physics.ucsb.edu; bazan@chem.ucsb.edu

DOI: 10.1002/adma.200802559

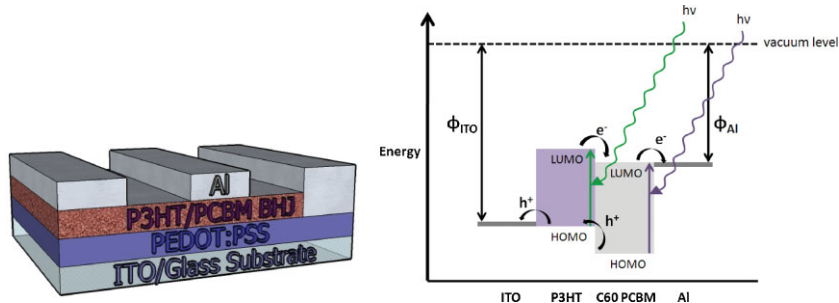


**Figure 1.** Left: device architecture of a typical bulk-heterojunction solar cell. The PEDOT:PSS hole-injection layer and P3HT/PCBM active layer are spin cast onto an ITO-coated glass substrate, followed by vapor deposition of the aluminum cathode. The thicknesses of the P3HT/C<sub>61</sub>-PCBM active layer and the PEDOT:PSS hole-injection layer are of order 100 nm and 50 nm, respectively. Right: energy-level diagram of a P3HT:C<sub>61</sub>-PCBM BHJ solar cell showing charge generation and transfer between the two organic components to the electrodes.

likely unique for each donor/acceptor system, and remains to be fully described for any one system.<sup>[7,8]</sup> Despite the fact that the blend nanomorphology is difficult to control or predict, the combination of empirical processing/performance relationships with morphological and optoelectronic characterization has resulted in device PCEs approaching 6%.<sup>[9,10]</sup> We seek here to describe some of the relationships between solution casting methodology, device morphology, and solar-cell performance that have been observed over the past several years, as research groups have endeavored to maximize device PCE. We will also make connections between some of the most effective techniques for device fabrication and discuss how the progress thus far might be extended to polymer BHJ systems in the future.

## 2. Device Design and Operating Principles

The device architecture and approximate energy-level diagram for a typical BHJ polymer solar cell are illustrated in Figure 1. A conductive hole-injection layer with a work function less than the highest occupied molecular orbital (HOMO) of the absorbing polymer is solution-deposited on top of the substrate. This is followed by the BHJ active layer, which consists of an interpenetrating network of a polymeric electron donor/hole acceptor and a fullerene-based electron acceptor/hole donor. In the most widely used plastic-solar-cell configuration, the substrate is indium-doped tin oxide-coated glass, the hole injection material is polyethylene dioxythiophene doped with polystyrene sulfonate (PEDOT:PSS), the active layer consists of an interpenetrating phase-separated network of poly(3-hexyl thiophene) (P3HT) and [6,6]-phenyl C<sub>61</sub>-butyric acid methyl ester (C<sub>61</sub>-PCBM), and the cathode is vapor-deposited aluminum.

In an operating solar cell, the absorption of solar photons occurs in both the polymer and the fullerene domains, and in either case results in a bound electron/hole pair known as an exciton. Recombination of the exciton is prevented via ultrafast exciton dissociation at the interface between the polymer and the fullerene. Once the dissociated electrons and holes leave the donor/acceptor interface, they are free to drift and diffuse (electrons to the low-work-function electrode and holes to the high-work-function electrode) due to the electric field created by the asymmetric electrodes. While several research groups have

successfully fabricated devices entirely processed from solution, in the majority of studies only the hole-injection layer and active layer are solution processed in order to facilitate the study of the active layer.<sup>[11]</sup> Figure 2 illustrates what efficiencies should be possible for polymer BHJ solar cells using C<sub>61</sub>-PCBM as the electron acceptor/hole donor.<sup>[3]</sup> There are a number of excellent in-depth reviews in the literature covering device-fabrication methods, material selection, and device physics.<sup>[1,12–16]</sup>

When designing new polymers for solar cells, a number of critical decisions have to be made while keeping in mind optimum solar cell performance, device lifetime, and commercial viability. The first decision is that of the absorbing donor polymer. To take advantage of

the full solar spectrum while maximizing device open-circuit voltage, the polymer absorption edge should be somewhere between 700–1000 nm. The difference between the lowest unoccupied molecular orbitals (LUMO) of the polymer and fullerene should be minimized in order to maximize the open-circuit voltage.<sup>[3,12]</sup> Additionally, the solid-state packing, solubility, miscibility with the fullerene, and carrier mobility must all be optimized to increase the efficiency of free-carrier generation and collection, and thereby increase the device short-circuit current and fill factor. Similar considerations regarding absorption and nanoscale phase separation should be made when choosing the acceptor material, although a relatively small number of soluble fullerene derivatives have dominated the field thus far. The materials that have yielded high-efficiency BHJ solar cells and are discussed in this article are illustrated in Figure 3.<sup>[1,9,17]</sup>

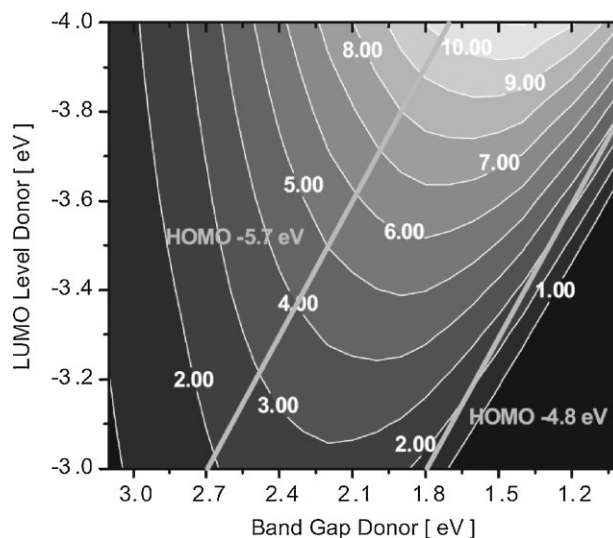


**Figure 2.** Using reasonable assumptions of energy losses and device fill factors, it is possible to calculate the maximum attainable PCE for a given polymer combined with C<sub>61</sub>-PCBM. This contour plot shows the calculated energy-conversion efficiency (contour lines and colors) versus the band-gap and the LUMO level of the light-absorbing polymer. Reproduced with permission from [3].

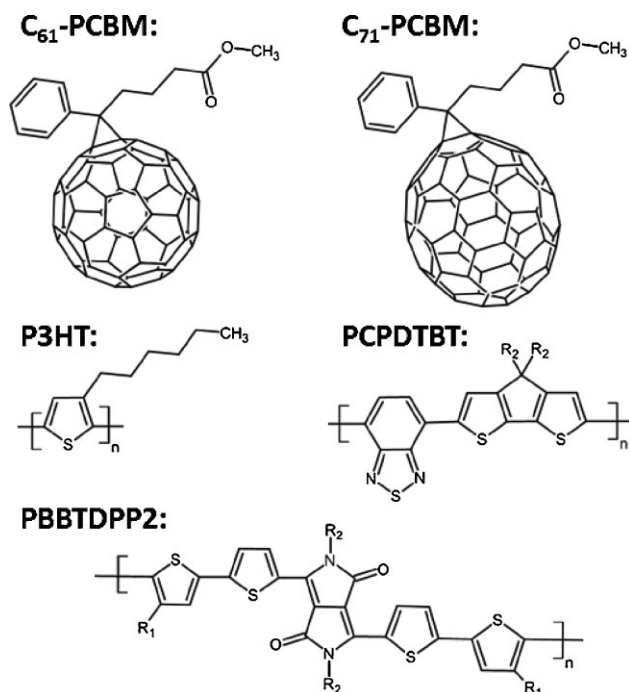


**Figure 3.** Several materials that have been used as active-layer components in high-efficiency bulk heterojunction solar cells.  $R_1$  indicates an n-dodecyl group and  $R_2$  indicates an ethyl-hexyl group.

Beyond basic material selection, however, lies a vast array of parameters that must be carefully controlled. While there are a number of methods for casting high-quality BHJ films from solution, they all must be optimized to control the interaction of the nascent film with the substrate, the solvent-evaporation kinetics, the deposition temperature, and the solvation environment during film formation. These factors, regardless of the specific deposition method, will ultimately determine the carrier mobility of the solar-cell active-layer materials, the degree of electron delocalization within the polymer, and the degree of interpenetration of the phase-separated domains. The nanoscale morphology can significantly affect losses due to exciton relaxation, geminate recombination, and free-carrier recombination.<sup>[12]</sup> In addition, architectural features, such as specialized electrodes for optimized charge injection, tandem solar cell structures, and encapsulation techniques, can also be beneficial to performance.<sup>[10,18]</sup> We describe below some of the techniques for controlling the solution-processing conditions that have proven successful for optimizing the BHJ morphology and obtaining some of the highest power-conversion efficiencies observed.

### 3. Methods for Optimizing the BHJ Nanomorphology

The great majority of BHJ-solar-cell fabrication up to this point has employed spin casting as the method for fabricating the polymer layers. While spin casting is not applicable as a large-scale manufacturing method, the process is simple, can be accomplished with small batches of material, and is widely reproducible. Surprisingly, film morphologies obtained from

spin casting translate well to other film-casting techniques such as doctor blading.<sup>[19]</sup> While every film-casting method will ultimately have its own set of adjustable parameters, the resulting morphology will depend on factors that will be present in any solution-casting technique. By understanding how each optimization technique fundamentally affects the film-deposition process, similar results might be reproduced on a larger scale using a fundamentally different method of film casting.

One of the earliest and most widely used methods of morphology control in BHJ solar cells is thermal annealing.<sup>[20]</sup> Heating active-layer films can, in certain systems, dramatically increase charge-carrier mobility and improve carrier collection by increasing order and coarsening the polymer and fullerene domains. This technique has proven most effective with polymers such as P3HT, which have demonstrable crystalline order. After film deposition, the devices can be heated (below the melting point) so that crystalline domains grow, thereby increasing carrier mobility and enhancing the connectivity of the polymer/fullerene interpenetrating network. For a P3HT/ $C_{61}$ -PCBM solar cell, the efficiency can increase from 0.83% to nearly 5% upon heating the film at 150 °C for 30 minutes.<sup>[20]</sup> The enhancement of desirable phase separation by thermal annealing was first imaged using transmission electron microscopy (TEM); subsequent Fourier-transform analysis of the images confirmed phase separation on both the meso- (>100 nm) and nanoscales (<20 nm).<sup>[20,21]</sup> In Figure 4, atomic force microscopy (AFM) and conducting-AFM images of P3HT/ $C_{61}$ -PCBM BHJ film cross sections show the evolution of mean domain sizes within the bulk of the film from 8 nm to 12 nm upon thermal annealing.<sup>[22]</sup> The scale of the phase separation shown in P3HT/ $C_{61}$ -PCBM is much smaller than has been observed in some other polymer systems, but greater levels of phase separation degrades device performance by forming pure domains so large that excitons cannot reach a donor/acceptor heterojunction interface prior to decay to the ground state.<sup>[15]</sup> The increase in polymer order has been demonstrated via X-ray diffraction by several groups.<sup>[20,23]</sup> It has proven difficult, however, to disentangle the effects of increased polymer order, changes to the interpenetrating network morphology, and changes to the local electronic environment at the interfaces within the device.

Despite compelling claims that the beneficial effects of annealing are simply to increase carrier mobility and improve the BHJ network morphology, recent work on the ultrafast transient absorption of P3HT/fullerene blends indicated that interfacial effects within the BHJ film may dominate the changes in device performance.<sup>[24,25]</sup> This work, along with that by a number of other groups, indicates that one of the primary modes by which annealing increases performance is by reducing geminate recombination of the recently dissociated exciton at the donor/acceptor interface.<sup>[26,27]</sup> A model has been proposed where ordered regions grow within the polymer domains that have a lower band-gap, and thus possess a higher HOMO level, than polymer at a disordered interface.<sup>[25]</sup> This higher HOMO level within the bulk of the polymer domain serves as a driving force for hole transfer, and thereby significantly decreases geminate recombination. While determining exactly what aspects of thermal annealing benefit the device is an active area of research, it is clear that i) increased P3HT order is crucial for optimum device performance, and ii) controlled phase separation

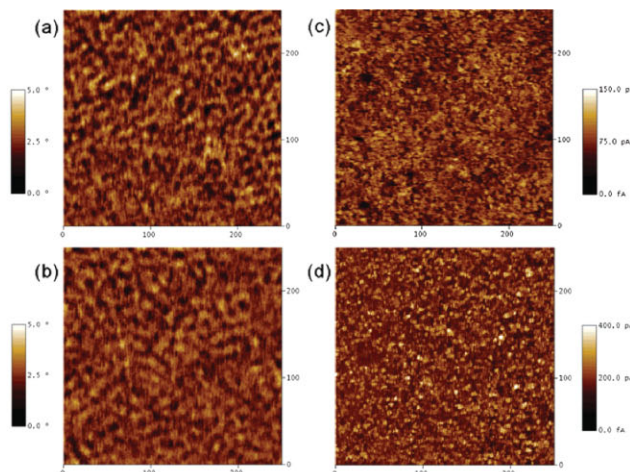
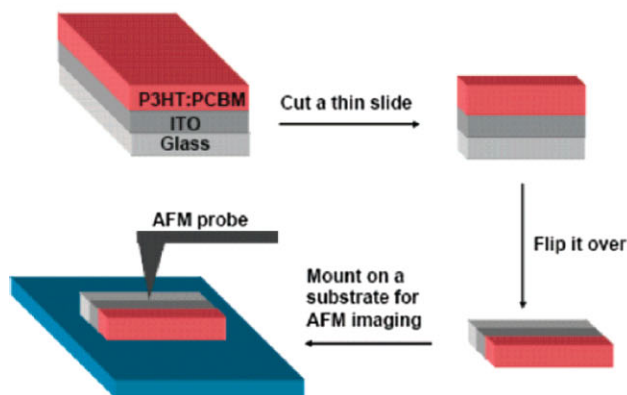


**Figure 4.** Imaging of the cross-section of a BHJ P3HT/C<sub>61</sub>-PCBM film can be accomplished using a focused ion beam and micromanipulator to prepare the sample. A schematic of how the sample is prepared is shown on the left. a,b) Phase images (250nm on a side) are shown along with current images obtained from c,d) conducting-AFM of the cross-sections (250nm on a side) a,c) before thermal annealing and b,d) after thermal annealing. Reproduced with permission from [22]. Copyright 2008 American Chemical Society.

is desired in the blend morphology to ensure continuous pathways to the electrodes; however, phase separation exceeding the polymer exciton diffusion length of about 10 nm can result in exciton relaxation to the ground state prior to reaching a polymer/fullerene interface.

As an alternative to thermal annealing, a set of techniques for active-layer morphology control and optimization has been reported, known as slow drying or solvent annealing.<sup>[28–30]</sup> P3HT/C<sub>61</sub>-PCBM solar cells processed by this technique can reach PCEs of 4.4%.<sup>[28]</sup> This technique uses a solvent with slightly higher boiling point and a controlled set of spin-coating conditions, such that not all of the solvent evaporates prior to removal of the device from the spin-coater. Reduced spin speeds combined with shorter spin times significantly slow the solvent-evaporation kinetics. Additionally, the device can be placed in an enclosed container in which the atmosphere rapidly saturates with solvent. In this way, the film-formation kinetics can be slowed further. This decreased rate of film formation, like thermal annealing, leads to improved interpenetration of the polymer and fullerene domains as well as increased order within the polymer domains. While thermal annealing has the distinct benefit that it can be used regardless of the film-deposition technique, slow-drying concepts could easily be employed when casting films by doctor blading or other methods.

As a comparable alternative to slow drying, certain additives with very high boiling points can be incorporated into the polymer/fullerene solution to reduce the drying kinetics without the need to remove the device from the spin coater or use an enclosed atmosphere during film formation.<sup>[9,31–36]</sup> 1,8-octanedithiol, 1,8-diiodooctane, nitrobenzene, chloronaphthalene, and other additives have been used to obtain high-efficiency solar cells (PCEs up to 4–5.5%) without any processing beyond the standard spin-coating procedure.<sup>[9,34–36]</sup> In the case of 1,8-octanedithiol and 1,8-diiodooctane, which are better solvents for the fullerene than the polymer, the effect is to dramatically increase aggregation and order within the polymer

domains while avoiding excessive crystallization of the fullerene. The selective solubility of the fullerene component in the additive is demonstrated in Figure 5, in which the absorption spectrum obtained from a PCPDTBT/C<sub>71</sub>-PCBM (structures shown in Fig. 3) BHJ film soaked in 1,8-octanedithiol is nearly identical to that obtained from a film of only PCPDTBT. These processing additives enable a gradual decline in the polymer solvent quality during evaporation, which can lead to a more thermodynamically preferred morphology. In the case of chloronaphthalene, which is a good solvent for both the polymer and fullerene, the only effect is to reduce the evaporation kinetics and allow additional crystallization of the polymer and phase separation between the

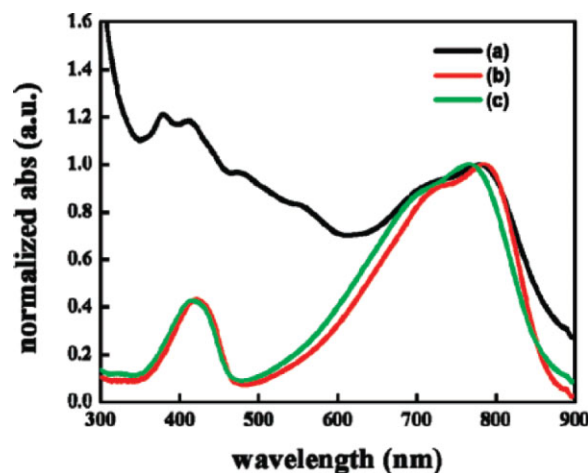


**Figure 5.** UV-vis absorption spectra of PCPDTBT/C<sub>71</sub>-PCBM films processed with 1,8-octanedithiol a) before removal of C<sub>71</sub>-PCBM with 1,8-octanedithiol and b) after removal of C<sub>71</sub>-PCBM with 1,8-octanedithiol, compared to the absorption spectrum of c) pristine PCPDTBT film. Reproduced with permission from [34]. Copyright 2008 American Chemical Society.

polymer and fullerene. In both mechanisms, nanoscale phase segregation can lead to control of the film morphology and enhanced device performance.

An added benefit of the additive approach is that it enables active-layer morphology optimization with polymers that do not readily crystallize by thermal annealing or realistically slow evaporation. In some cases, the shift in solvent quality leads to levels of interchain order that seemingly cannot be obtained by other means.<sup>[9,37]</sup> This is especially evident in certain low-band-gap polymer systems that do not show a crystallization peak by differential scanning calorimetry, but that must have some local order, as evidenced by significant variations in the absorption onset. This technique was used to achieve more than 5.5% PCE in a solar cell based on PCPDTBT with C<sub>71</sub>-PCBM, compared to the 3–4% PCE observed when additives were not used.<sup>[9]</sup> The effect of 1,8-octanedithiol on the external quantum efficiency, also known as incident-photon conversion efficiency, of a PCPDTBT/C<sub>71</sub>-PCBM solar cell is shown in Figure 6, and compared to the effect of thermal annealing on a P3HT/C<sub>61</sub>-PCBM solar cell. While the annealed P3HT-based device has greater peak efficiency, the increased breadth of the PCPDTBT-based solar cell absorption results in increased short-circuit current and a more efficient device. By controlling the solvent quality of the additive for both the polymer and the fullerene, both the polymer order and the degree of phase separation can be controlled independently in order to maximize device performance.

Several recent papers have used solvent mixtures in a different way.<sup>[17,36,38]</sup> In these approaches, poor-quality solvents were mixed with good solvents to induce aggregation or nanofiber formation in the solvent prior to film casting. In a recent paper, the low-band-gap polymer PBDTDP2, shown in Figure 3, was dissolved in a solvent mixture that partially aggregated the polymer in solution. By promoting polymer order in this way, the system yielded 4% PCE.<sup>[17]</sup> The performance of PBDTDP2/C<sub>71</sub>-PCBM solar cells can be optimized to some degree by either

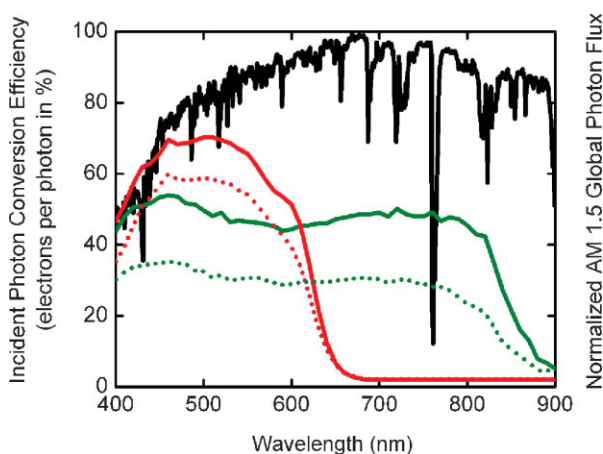


**Figure 6.** External quantum efficiency spectra of polymer BHJ solar cells composed of P3HT/C<sub>61</sub>-PCBM before (dotted red line) and after (solid red line) thermal annealing, and PCPDTBT/C<sub>71</sub>-PCBM with (solid green line) and without (dotted green line) the use of 1,8-octanedithiol. The AM 1.5G reference spectrum is shown in black. Reproduced with permission from [9]. Copyright 2007 Nature Publishing Group.

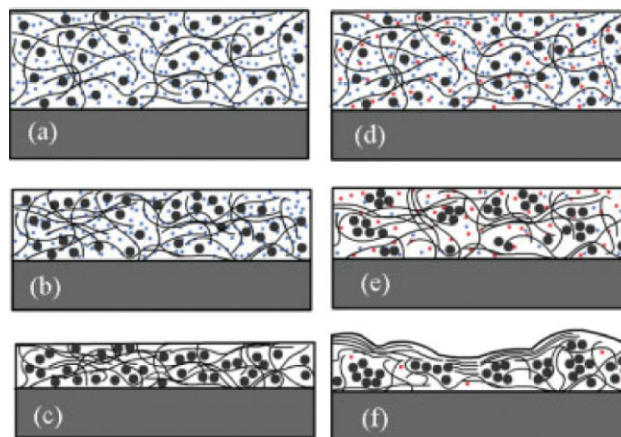


**Figure 7.** Illustration of nanoscale phase separation during spin-coating. The black lines represent P3HT polymer chains and the large black circles are C<sub>61</sub>-PCBM. a–c) Correspond to the evolution of the spin-coated film when 1,2-dichlorobenzene (small blue dots) is the sole solvent; d–f) correspond to the progression when n-octanedithiol (small red dots) is added into the 1,2-dichlorobenzene. Reproduced with permission from [32].

thermal annealing or by the use of mixed solvents, but the highest-efficiency devices utilized mixed solvents.

The use of very-slow-drying solvent additives often results in some vertical phase separation in which the polymer concentration will be greater at the film/air interface and the fullerene concentration will be greater at the film/substrate interface.<sup>[31]</sup> This effect was studied by removing a P3HT/C<sub>61</sub>-PCBM BHJ film from the substrate and using X-ray photoelectron spectroscopy to determine the sulfur-to-carbon ratio on the top and bottom surfaces. An illustration of the proposed evaporation and vertical-phase-separation process is shown in Figure 7. The segregation can occur by any solution-casting method, but it is accentuated by the decreased evaporation kinetics associated with additive processing, which can lead to more energetically favored interface compositions.<sup>[39]</sup> In the ideal structure for device performance, the polymer should be more prevalent at the anode and the fullerene more prevalent at the cathode; thus, the observed vertical phase separation is nonoptimal. This issue has been approached in one publication by creating an inverted device structure with a cesium carbonate cathode deposited on top of the active layer and a vanadium oxide anode deposited on top of the substrate. This inverted structure led to a P3HT/C<sub>61</sub>-PCBM solar cell that was 4.2% efficient when optimized.<sup>[40]</sup> Another approach was to synthesize a fullerene derivative with a fluorinated octyl branch that self-segregates to the film/air interface; this technique increased the performance of a P3HT/C<sub>61</sub>-PCBM solar cell from 3.1 to 3.8% PCE.<sup>[41]</sup> Both approaches are significant steps towards using energetically preferred interfacial compositions to improve device performance.

When considering how to create the optimum bulk-heterojunction morphology, the idea of using controlled self-assembly via surface energies and equilibrium phase separation is appealing in terms of device performance, thermal stability, and device lifetime. To that end, some effort has been directed toward self-assembling block-copolymer systems with both chromophore- and fullerene-functionalized blocks.<sup>[42–44]</sup> To date,

the scale of the phase separation for these block-copolymer systems has yet to reach significantly below the exciton diffusion length of the polymers. Future advances in block-copolymer synthesis and design are likely to lead to finer-scale phase separation and higher-performance devices. As a compelling example, we note the use of a diblock-copolymer in which one block was functionalized with P3HT-like domains and the other was functionalized with fullerene-like domains for use as a compatibilizer mixed into a P3HT/C<sub>61</sub>-PCBM BHJ solar cell.<sup>[45]</sup> While the initial device efficiencies were comparable at around 2.5%, the device utilizing the compatibilizer could be heated at 140 °C for 10 h without any performance degradation, whereas the standard device performance dropped more than 40% under the same conditions.

#### 4. Progress in Printing Plastic Solar Cells

While predicting how various methods of device optimization will extend to large-scale production techniques is difficult, the fundamental concepts behind solvent evaporation rate, solvation environment during film formation, and the thermal behavior of the materials will still apply. The performance observed with spin-cast films of P3HT and C<sub>61</sub>-PCBM has been successfully extended to films prepared by doctor blading and inkjet printing.<sup>[19,46,47]</sup> A recent review discusses some of the different approaches to large-scale printing of polymer solar cells and what the key processing parameters are for each.<sup>[1]</sup>

The second most widely employed BHJ-film-deposition technique is doctor blading, a method in which the substrate is affixed to a temperature-controlled surface and a smooth blade sweeps across the surface with a bead of BHJ solution between the blade and the substrate.<sup>[48]</sup> This technique has been well optimized and ultimately leads to very similar film morphologies and levels of device performance as spin-coating. Solar cells based on P3HT and C<sub>61</sub>-PCBM in excess of 4% PCE have been fabricated by this technique combined with either thermal-annealing or mixed-solvent approaches.<sup>[19,46]</sup>

A related technique was recently described for creating solar cells by brush painting using a nylon-fiber brush.<sup>[49]</sup> The article reported greater than 5% PCE using P3HT and C<sub>61</sub>-PCBM by carefully controlling the substrate temperature and post-deposition thermal-annealing conditions. The increase in efficiency over films spin cast from the same materials was attributed to the alignment of the polymer chains during brush casting, leading to increased order in the polymer domains while the solvent-evaporation rate could be controlled by the substrate temperature.

Polymer solar cells cast by inkjet printing of the active layer have achieved performances as high as 3.5% PCE for a P3HT/C<sub>61</sub>-PCBM solar cell.<sup>[19,50,51]</sup> While there were several key differences in the optimum parameters relative to spin-coated or doctor-bladed films, the majority of the factors remained constant. Due to the tendency of highly regioregular P3HT to clog inkjet nozzles, the best devices were fabricated from P3HT that was only about 96% regioregular; in spin-cast devices, the optimum regioregularity is greater than 98%.<sup>[50]</sup> Additionally, unlike spin-cast films, low-boiling-point solvents with faster drying times yielded better performance than higher-

boiling-point solvents. The resulting films exhibited very rough active layers. However, the highest levels of performance were ultimately obtained using a mixed-solvent system with two solvents of different boiling points to minimize surface roughness while extending the film-formation time.

Spray coating has been used to obtain solar cells with greater than 2.5% PCE using a P3HT/C<sub>61</sub>-PCBM BHJ blend.<sup>[52,53]</sup> The technique involves the use of air-brush-style paint guns (one for each of the two components, to enable independent control of the composition) and careful optimization of solvent, casting conditions, and thermal annealing conditions. This technique, like several of those described, has the potential to enable inexpensive solar cells that could be packaged in ways that other solar technologies could not consider.

#### 5. Conclusions and Outlook

Each of the film-casting methods described has a unique set of adjustable parameters, but the processing/structure/property relationships gleaned from spin casting have enabled relatively rapid optimization with some of these systems. Thermal annealing, slow drying, additive processing, and controlled self-assembly can each play a role in any solution-casting method. In order to adapt current optimization techniques to new film-casting methods, it will be important to understand the fundamental differences in solvent evaporation kinetics, viscosity effects, and shear stresses placed on the fluid during solvent evaporation. The existing techniques used to optimize the BHJ active-layer morphology can then be combined with the techniques associated with novel casting methods in order to maximize performance. By controlling the polymer absorption and local order, the polymer/fullerene miscibility, the solvent evaporation kinetics, and the solvation environment during film formation, it will be possible to fabricate high-efficiency solar cells by a variety of large-scale printing methods in the future.

#### Acknowledgements

The authors gratefully acknowledge the Office of Naval Research and the Institute for Collaborative Biotechnologies for financial support of our programs. J.P. thanks the NDSEG fellowship for support. This article is part of a special issue on Interfaces in Organic Electronics.

- [1] C. J. Brabec, J. R. Durrant, *MRS Bull.* **2008**, *33*, 670.
- [2] J. S. Huang, G. Li, Y. Yang, *Adv. Mater.* **2008**, *20*, 415.
- [3] M. C. Scharber, D. Wuhlbacher, M. Koppe, P. Denk, C. Waldauf, A. J. Heeger, C. L. Brabec, *Adv. Mater.* **2006**, *18*, 789.
- [4] G. Dennler, M. C. Scharber, T. Ameri, P. Denk, K. Forberich, C. Waldauf, C. J. Brabec, *Adv. Mater.* **2008**, *20*, 579.
- [5] C. D. Dimitrakopoulos, P. R. L. Malenfant, *Adv. Mater.* **2002**, *14*, 99.
- [6] Y. Y. Lin, D. J. Gundlach, S. F. Nelson, T. N. Jackson, *IEEE Electron Device Lett.* **1997**, *18*, 606.
- [7] C. Muller, T. A. M. Ferenczi, M. Campoy-Quiles, J. M. Frost, D. D. C. Bradley, P. Smith, N. Stingelin-Stutzmann, J. Nelson, *Adv. Mater.* **2008**, *20*, 3510.
- [8] B. Lei, Y. Yao, A. Kumar, Y. Yang, V. Ozolins, *J. Appl. Phys.* **2008**, *104*, 024504.

- [9] J. Peet, J. Y. Kim, N. E. Coates, W. L. Ma, D. Moses, A. J. Heeger, G. C. Bazan, *Nat. Mater.* **2007**, *6*, 497.
- [10] J. Y. Kim, K. Lee, N. E. Coates, D. Moses, T. Q. Nguyen, M. Dante, A. J. Heeger, *Science* **2007**, *317*, 222.
- [11] E. Ahlswede, W. Muhleisen, M. Wahi, J. Hanisch, M. Powalla, *Appl. Phys. Lett.* **2008**, *92*, 143307.
- [12] E. Bundgaard, F. C. Krebs, *Sol. Energy Mater. Sol. Cells* **2007**, *91*, 954.
- [13] B. C. Thompson, J. M. J. Frechet, *Angew. Chem. Int. Ed.* **2008**, *47*, 58.
- [14] S. Gunes, H. Neugebauer, N. S. Sariciftci, *Chem. Rev.* **2007**, *107*, 1324.
- [15] H. Hoppe, N. S. Sariciftci, *J. Mater. Chem.* **2006**, *16*, 45.
- [16] G. Li, V. Shrotriya, Y. Yao, J. S. Huang, Y. Yang, *J. Mater. Chem.* **2007**, *17*, 3126.
- [17] M. M. Wienk, M. Turbiez, J. Gilot, R. A. J. Janssen, *Adv. Mater.* **2008**, *20*, 2556.
- [18] M. D. Irwin, B. Buchholz, A. W. Hains, R. P. H. Chang, T. J. Marks, *Proc. Natl. Acad. Sci. USA* **2008**, *105*, 2783.
- [19] P. Schilinsky, C. Waldauf, C. J. Brabec, *Adv. Funct. Mater.* **2006**, *16*, 1669.
- [20] W. Ma, C. Yang, X. Gong, K. Lee, A. J. Heeger, *Adv. Funct. Mater.* **2005**, *15*, 1617.
- [21] W. Ma, C. Yang, A. J. Heeger, *Adv. Mater.* **2007**, *19*, 1387.
- [22] M. Dante, J. Peet, T. Q. Nguyen, *J. Phys. Chem. C* **2008**, *112*, 7241.
- [23] P. Vanlaeke, G. Vanhoyland, T. Aernouts, D. Cheyns, C. Deibel, J. Manca, P. Heremans, J. Poortmans, *Thin Solid Films* **2006**, *511*, 358.
- [24] I. W. Hwang, D. Moses, A. J. Heeger, *J. Phys. Chem. C* **2008**, *112*, 4350.
- [25] I. W. Hwang, C. Soci, D. Moses, Z. G. Zhu, D. Waller, R. Gaudiana, C. J. Brabec, A. J. Heeger, *Adv. Mater.* **2007**, *19*, 2307.
- [26] H. Ohkita, S. Cook, Y. Astuti, W. Duffy, S. Tierney, W. Zhang, M. Heeney, L. McCulloch, J. Nelson, D. D. C. Bradley, J. R. Durrant, *J. Am. Chem. Soc.* **2008**, *130*, 3030.
- [27] S. De, T. Pascher, M. Maiti, K. G. Jespersen, T. Kesti, F. L. Zhang, O. Inganas, A. Yartsev, V. Sundstrom, *J. Am. Chem. Soc.* **2007**, *129*, 8466.
- [28] G. Li, V. Shrotriya, J. S. Huang, Y. Yao, T. Moriarty, K. Emery, Y. Yang, *Nat. Mater.* **2005**, *4*, 864.
- [29] G. Li, Y. Yao, H. Yang, V. Shrotriya, G. Yang, Y. Yang, *Adv. Funct. Mater.* **2007**, *17*, 1636.
- [30] S. Miller, G. Fanchini, Y. Y. Lin, C. Li, C. W. Chen, W. F. Su, M. Chhowalla, *J. Mater. Chem.* **2008**, *18*, 306.
- [31] J. Peet, C. Soci, R. C. Coffin, T. Q. Nguyen, A. Mikhailovsky, D. Moses, G. C. Bazan, *Appl. Phys. Lett.* **2006**, *89*, 252105.
- [32] Y. Yao, J. H. Hou, Z. Xu, G. Li, Y. Yang, *Adv. Funct. Mater.* **2008**, *18*, 1783.
- [33] A. Pivrikas, P. Stadler, H. Neugebauer, N. S. Sariciftci, *Org. Electron.* **2008**, *9*, 775.
- [34] J. K. Lee, W. L. Ma, C. J. Brabec, J. Yuen, J. S. Moon, J. Y. Kim, K. Lee, G. C. Bazan, A. J. Heeger, *J. Am. Chem. Soc.* **2008**, *130*, 3619.
- [35] A. J. Moule, K. Meerholz, *Adv. Mater.* **2008**, *20*, 240.
- [36] F. C. Chen, H. C. Tseng, C. J. Ko, *Appl. Phys. Lett.* **2008**, *92*, 103316.
- [37] A. J. Moule, A. Tsami, T. W. Buennagel, M. Forster, N. M. Kronenberg, M. Scharber, M. Koppe, M. Morana, C. J. Brabec, K. Meerholz, U. Scherf, *Chem. Mater.* **2008**, *20*, 4045.
- [38] H. Xin, F. S. Kim, S. A. Jenekhe, *J. Am. Chem. Soc.* **2008**, *130*, 5424.
- [39] M. Campoy-Quiles, T. Ferenczi, T. Agostinelli, P. G. Etchegoin, Y. Kim, T. D. Anthopoulos, P. N. Stavrinou, D. D. C. Bradley, J. Nelson, *Nat. Mater.* **2008**, *7*, 158.
- [40] H. H. Liao, L. M. Chen, Z. Xu, G. Li, Y. Yang, *Appl. Phys. Lett.* **2008**, *92*, 173303.
- [41] Q. S. Wei, T. Nishizawa, K. Tajima, K. Hashimoto, *Adv. Mater.* **2008**, *20*, 2211.
- [42] C. Zhang, S. Choi, J. Haliburton, T. Cleveland, R. Li, S. S. Sun, A. Ledbetter, C. E. Bonner, *Macromolecules* **2006**, *39*, 4317.
- [43] S. S. Sun, C. Zhang, A. Ledbetter, S. Choi, K. Seo, C. E. Bonner, M. Drees, N. S. Sariciftci, *Appl. Phys. Lett.* **2007**, *90*, 043117.
- [44] S. S. Sun, *Sol. Energy Mater. Sol. Cells* **2003**, *79*, 257.
- [45] K. Sivula, Z. T. Ball, N. Watanabe, J. M. J. Frechet, *Adv. Mater.* **2006**, *18*, 206.
- [46] D. Muhlbacher, M. Scharber, M. Morana, Z. G. Zhu, D. Waller, R. Gaudiana, C. Brabec, *Adv. Mater.* **2006**, *18*, 2931.
- [47] T. Aernouts, T. Aleksandrov, C. Girotto, J. Genoe, J. Poortmans, *Appl. Phys. Lett.* **2008**, *92*, 033306.
- [48] F. Padinger, C. J. Brabec, T. Fromherz, J. C. Hummelen, N. S. Sariciftci, *Opto-Electron. Rev.* **2000**, *8*, 280.
- [49] S. S. Kim, S. I. Na, J. Jo, G. Tae, D. Y. Kim, *Adv. Mater.* **2007**, *19*, 4410.
- [50] C. N. Hoth, S. A. Choulis, P. Schilinsky, C. J. Brabec, *Adv. Mater.* **2007**, *19*, 3973.
- [51] C. N. Hoth, P. Scholonsky, S. A. Choulis, C. J. Brabec, *Nano Lett.* **2008**, *8*, 2806.
- [52] D. J. Vak, S. S. Kim, J. Jo, S. H. Oh, S. I. Na, J. W. Kim, D. Y. Kim, *Appl. Phys. Lett.* **2007**, *91*, 081102.
- [53] R. Green, A. Morfa, A. J. Ferguson, N. Kopidakis, G. Rumbles, S. E. Shaheen, *Appl. Phys. Lett.* **2008**, *92*, 033301.